HHS Public Access

Author manuscript

J Int Soc Respir Prot. Author manuscript; available in PMC 2018 November 27.

Published in final edited form as:

J Int Soc Respir Prot. 2017 ; 34(1): 40–57.

Development of a Manikin-Based Performance Evaluation Method for Loose-Fitting Powered Air-Purifying Respirators

Mike Bergman[*], **Rohan Basu**, **Zhipeng Lei**, **George Niezgoda**, and **Ziqing Zhuang**

National Institute for Occupational Safety and Health, National Personal Protective Technology Laboratory, Pittsburgh, Pennsylvania 15236

Abstract

Objective: Loose-fitting powered air-purifying respirators (PAPRs) are increasingly being used in healthcare. NIOSH has previously used advanced manikin headforms to develop methods to evaluate filtering facepiece respirator fit; research has now begun to develop methods to evaluate PAPR performance using headforms. This preliminary study investigated the performance of PAPRs at different work rates to support development of a manikin-based test method.

Methods: Manikin penetration factors (mPF) of three models of loose-fitting PAPRs were measured at four different work rates (REST: 11 Lpm, LOW: 25 Lpm, MODERATE: 48 Lpm, and HIGH: 88 Lpm) using a medium-sized NIOSH static advanced headform mounted onto a torso. In-mask differential pressure was monitored throughout each test. Two condensation particle counters were used to measure the sodium chloride aerosol concentrations in the test chamber and also inside the PAPR facepiece over a 2-minute sample period. Two test system configurations were evaluated for returning air to the headform in the exhalation cycle (filtered and unfiltered). Geometric mean (GM) and 5th percentile mPFs for each model/work rate combination were computed. Analysis of variance tests were used to assess the variables affecting mPF.

Results: PAPR model, work rate, and test configuration significantly affected PAPR performance. PAPR airflow rates for the three models were approximately 185, 210, and 235 Lpm. All models achieved GM mPFs and 5^{th} percentile mPFs greater than their designated Occupational Safety and Health Administration assigned protection factors despite negative minimum pressures observed for some work rate/model combinations.

Conclusions: PAPR model, work rate, and test configuration affect PAPR performance. Advanced headforms have potential for assessing PAPR performance once test methods can be matured. A manikin-based inward leakage test method for PAPRs can be further developed using the knowledge gained from this study. Future studies should vary PAPR airflow rate to better understand the effects on performance. Additional future research is needed to evaluate the correlation of PAPR performance using advanced headforms to the performance measured with human subjects.

[*]Corresponding author: MBergman@cdc.gov.

Disclaimer

The findings and conclusions of this article are those of the authors and do not necessarily represent the views of the National Institute for Occupational Health and Safety. Mention of a commercial product or trade name does not constitute endorsement by the National Institute for Occupational Safety and Health.

Keywords

powered air-purifying respirator; PAPR; NIOSH-approved respirator; respirator performance

INTRODUCTION

Powered air-purifying respirators (PAPRs) use a battery powered motorized fan to draw air through an air-purifying element (particulate filter and/or sorbent cartridge) and supply it to a respiratory inlet covering (RIC), such as a helmet, loose-fitting facepiece (LFF) (forming a partial seal to the face), hood (completely covering the head and neck and may also incorporate a shroud to cover portions of the shoulders and torso), or elastomeric facepiece. The airflow rate can be constant or variable (as for breath-assisted PAPRs), however, the blower motor must deliver a minimum of 170 liters/minute (Lpm) (LFF) or 115 Lpm (tight-fitting) to meet National Institute for Occupational Safety and Health (NIOSH) approval requirements.(Federal Register 1995) PAPRs are used in both industrial workplaces and healthcare settings.(Bureau of Labor Statistics and National Institute for Occupational Safety and Health 2003) The 2003 severe acute respiratory syndrome (SARS) outbreak and 2009 H1N1 influenza pandemic highlighted the ongoing need for effective respiratory protection for healthcare workers (HCWs).(Khoo, Leng et al. 2005, Liverman, Domnitz et al. 2014, Wizner, Stradtman et al. 2016) In healthcare settings, PAPRs with RICs covering the face and eyes have the additional benefit of reducing exposure to infectious body fluid droplet sprays. Shrouds covering the neck, shoulders, and/or chest can provide an additional spray barrier. Loose-fitting PAPRs (both LFF and hoods) are an attractive option because they do not require fit testing.(Liverman, Domnitz et al. 2014)

The air supply from the PAPR motor creates positive pressure inside the RIC to prevent the infiltration of contaminated ambient air; however, PAPRs are not “positive-pressure” devices (in terms of NIOSH approval) because they are not tested by NIOSH to maintain positive pressure. The assigned protection factor (APF) is the expected level of protection provided to the user by a respirator used under the program requirements of a respiratory protection program defined by the Occupational Safety and Health Administration (OSHA).(OSHA 1998, OSHA 2006) The APF for PAPRs depends on the type of RIC and ranges from 25 (using a LFF or loose-fitting hood) to 1,000 (for a tight-fitting full-facepiece, or for a loose-fitting hood which has been demonstrated by the manufacturer to have protection performance of ≥ 1,000.(OSHA 2006) While supplied airflow rates of loose-fitting PAPRs have been measured in the range of 170–237 Lpm, peak inhalation flows (PIF) of adults exercising at heavy work rates can exceed 300 Lpm.(Cohen, Hecker et al. 2001, Berndtsson 2004, Janssen, Anderson et al. 2005, Anderson, Casidy et al. 2006, Martin, Moyer et al. 2006) Because the wearer may require a higher inhalation flow rate than can be supplied, a negative pressure inside the facepiece could result (a condition referred to as “over breathing”); thus, in the over breathing condition of loose-fitting PAPRs there is a potential for contaminated air to enter the RIC during these short time spikes.(Mackey, Johnston et al. 2005)

Studies using manikin heads or actual respirator wearers have been designed to assess PAPR performance in terms of reducing the amount of airborne contaminants to which a user may be exposed. Simulated workplace protection factor (SWPF) is a surrogate measure of the workplace protection provided by a respirator.(NIOSH 2005) SWPF studies are laboratory-based in which subjects perform exercises that simulate workplace activities. Workplace protection factor (WPF) is a measure of the protection provided in the workplace by a properly functioning respirator when correctly worn and used.(NIOSH 2005) WPF studies are performed in actual workplaces where respirator performance is assessed during work activities. Gao et al. (2016)(Gao, McKay et al. 2016) evaluated performance using a manikin headform wearing either properly sized, improperly sized, or stretched-out (elastic neck band) PAPR LFFs. Testing was performed at mean inspiratory flowrates of 30, 55, 85, and 135 Lpm with cyclic breathing. Higher particle leakage was found at higher flow rates for all hood conditions; the most leakage was observed for the stretched-out hood. Cohen et al. (2001)(Cohen, Hecker et al. 2001) evaluated SWPFs of test subjects wearing five different loose-fitting PAPR models (four with a hood/helmet, and one with a loose-fitting hood) and observed SWPFs from 240 to ≥ 250,000, indicating a high level of performance. Koivisto et al. (2015)(Koivisto, Aromaa et al. 2015) evaluated a PAPR model with a LFF worn by workers while coating components with TiO_2 or CuxOy nanoparticles using a flame spray process and derived protection factors > 1×10^6.

The current NIOSH approval test requirements for PAPRs (42 CFR Part 84)(Federal Register 1995) (isoamyl acetate fit evaluation, airflow testing, inhalation and exhalation resistance (for tight-fitting facepieces only), silica dust loading test, and noise level assessment) were based on industrial use needs. NIOSH is currently working on efforts to update PAPR approval standards to accommodate developments in design and technology. This, in turn, may lead to PAPR designs with higher acceptability for the healthcare setting, such as reduced weight, bulk, and a quieter motor. Research is needed to improve existing test methods and to develop new test methods for evaluating PAPR performance. This study presents the results of preliminary performance experiments using a sodium chloride test aerosol to investigate developing a manikin-based test method.

MATERIALS AND METHODS

PAPR Models

Three popular PAPR models used in healthcare were evaluated. All models were configured with a loose-fitting RIC): 1) 3M Air-Mate™ with model BE-12 facepiece (size regular) (3M Company, St. Paul, MN) (OSHA APF = 25), 2) MaxAir® Systems 78SP-36 cuff system with disposable cuff (size M/L) (Bio-Medical Devices, Inc., Irvine, CA) (OSHA APF = 25), and 3) Sentinel XL™ with S-2019-10 hood (size M/L) (ILC Dover, LP), Frederica, DE) (OSHA APF = 1,000).(ILC Dover LP 2011) The model configurations differ in several design aspects (Fig. 1). The Air-Mate™ and Sentinel XL™ units both have an external blower/filter unit and a hose for delivery of filtered air to the RIC. The MaxAir® model is a helmet design where both the filter and blower motor are contained in the helmet. The LFF tested with the Air-Mate™ unit has an elastic cuff at the neck/chin area. The MaxAir® configuration is also an LFF with an elastic neck cuff design which attaches to the helmet

with a zipper. The Sentinel XL™ model has a hood with an inner elastic neck cuff and also has a double shroud design (i.e., an inner and outer shroud extending over the shoulders). As specified in the user manual, the inner shroud should be tucked into a user's outer garment (e.g., lab coat or coveralls), while the outer shroud lays over the outside of the garment. The MaxAir® model had three airflow settings (low, medium, and high); for these experiments the low setting was used. Both the Air-Mate™ and Sentinel XL™ models only had one airflow setting.

Inward Leakage Test Chamber

Inward leakage (IL) of contaminants into a respirator RIC can occur by penetration through an air-filtering element, through the face seal area (for tight-fitting RICs), across the gap between a loose-fitting RIC and the user's face, or through leaks in components such as hose connections, valves, RIC seams, etc. Inward leakage testing of generated sodium chloride (NaCl) aerosol was performed in an acrylic test chamber (l, w, h: 30" × 36" × 72") equipped with mixing fans and an exhaust port (Fig 2). The aerosol was generated using a six-jet Collison nebulizer (BGI Incorporated, Waltham, MA) with 2 w/v % NaCl solution in deionized water. The aerosol was passed through a diffusion drier and then a Kr-85 neutralizer (model: 3054, TSI, Inc., Shoreview, MN) before dispersion into the chamber. High efficiency particulate air (HEPA)-filtered dilution air was added to the chamber at the rate of 2–5 Lpm to maintain an aerosol concentration of $2.0–2.5 \times 10^5$ particles/cm^3. The chamber NaCl particle distribution was measured with a scanning mobility particle sizer spectrometer (SMPS) (model: 3936, TSI Inc.) system consisting of a classifier controller (model: 3080, TSI, Inc.), a differential mobility analyzer (DMA) (model: 3081, TSI, Inc.), a condensation particle counter (CPC) (model: 3772, TSI, Inc.), and an aerosol neutralizer (model: 3077A, TSI, Inc.). Data from four SMPS scans were averaged to characterize the aerosol as having a count median diameter (CMD) of 80.6 nm and geometric standard deviation (GSD) of 1.8.

PAPRs were mounted onto a medium-sized static advanced headform which was mounted onto a clothing display torso. The medium size represents the head and face shape of approximately 50% of the current U.S. workforce.(Zhuang, Benson et al. 2010) The headform has silicone elastomer skin and variable tissue depth at defined locations throughout the face to better simulate the respirator fit of people.(Bergman, Zhuang et al. 2014, Bergman, He et al. 2015) The torso was dressed with an undershirt and a poly cotton blend lab coat. A breathing tube (22 mm ID) ran from the inside of the headform's mouth, out of the mid back of the torso, and was connected to an isolated breathing lung outside of the chamber. The breathing lung contained a 4 liter neoprene expandable bladder from which air cyclically flowed back and forth to the headform. A hose connected a separate port on the breathing lung to a breathing simulator (model: BRSS, Koken Ltd., Japan). Cyclically flowing air from the breathing machine caused the bladder to inflate and deflate. This configuration prevented any particles potentially generated by the simulator from traveling to the PAPR RIC and being erroneously counted in the IL measurement (Fig 2).

Two configurations of returning the air from the bladder back to the headform (i.e., the exhalation circuit) were evaluated. The first configuration, referred to as HEPA-CONFIG,

utilized 2 two-way non-return valves and an in-line-HEPA filter to provide filtered air back to the headform (Fig 2). This configuration was evaluated on the notion that even though PAPRs have been shown to have high performance, the particle concentration inside the breathing pathway could potentially build over the two minute test duration and cause an erroneously elevated particle measurement inside the RIC. The second configuration, referred to NO-HEPA-CONFIG, where the HEPA filter and two-way valves were removed, was evaluated to compare the results to the HEPA-CONFIG. In the NO-HEPA-CONFIG, air flowed directly to and from the bladder through the same hose and was not filtered in the exhalation cycle.

IL testing was performed at four minute ventilations (V_E) using the following breathing rates (breaths/min (f)) and tidal volumes (V_T): REST (V_E = 11 Lpm, f =14, V_T = 0.8 L), LOW (V_E = 25 Lpm, f =21, V_T = 1.2 L), MODERATE (V_E = 48 Lpm, f =28, V_T = 1.7 L), HIGH (V_E = 88 Lpm, f =38, V_T = 2.3 L). Minute ventilations for men and women performing various work tasks are well summarized.(Adams 1993, Caretti and Coyne 2004, Ainsworth BE, Haskell WL et al. 2011) The four work rates were chosen to provide a wide range of respiration from sedentary to heavy exertion. Mean V_E values similar to those selected for this study were observed by Sinkule et al. (2016)(Sinkule, Powell et al. 2016) for subjects wearing PAPRs (three models of loose-fitting and one model of tight-fitting) at REST and while walking for four minutes on a treadmill at oxygen consumption (VO_2) rates of 1.0 Lpm (LOW), 2.0 Lpm (MODERATE), and 3.0 Lpm or maximum (HIGH). A V_E of 11 Lpm is considered to be sedentary and in the range of sitting and standing.(Adams 1993) A V_E of 25 is in the range of light work which might represent standing or working in an operating room and carrying weight < 25 lbs. (3.5 metabolic equivalent of task (METS))(Ainsworth BE, Haskell WL et al. 2011) A V_E in the range of 45 Lpm can represent moderate exertion, as might be expected in lifting or moving patients (i.e., weight > 100 lbs., 8.5 METS). (Ainsworth BE, Haskell WL et al. 2011) A V_E in the range of 85 Lpm represents heavy work as during running at seven miles per hour (11.0 METS) (Ainsworth BE, Haskell WL et al. 2011), which might be experienced in running on an emergency call.

Inward leakage measurements were taken using two condensation particle counters (CPC) (model: 8022A; TSI, Inc.) and two laptop computers with Aerosol Instrument Manager® software (V.9.0.0.0, TSI, Inc.). One CPC sampled the chamber NaCl aerosol concentration (Cout) at a location ~2 cm in front of the PAPR hood (i.e., outside of the hood) at the level of the headform's mouth. The other CPC sampled the NaCl aerosol concentration inside the RIC (C_{in}). The model 8022A CPC has an accuracy of +/− 10% up to 5×10^5 particles /cm^3 as specified by the manufacturer. Both CPCs were set to sample in low flow mode (300 cm^3/min). Equal lengths of tubing (model: Tygon S3 E3603 NSF, ~1.22 m, ID 6.4 mm; Saint Gobain Performance Plastics, Charny, France) were used to transport the aerosol to each CPC. For each test, each CPC collected a 2-min sample at the rate of one data point / second. Each CPC reported the average concentration of the 2-min sample which was later used for data analysis. The in-mask measurement was accomplished by connecting a rigid plastic tube ~3–5 cm long (depending on the PAPR model) to the sample tubing and extending it through the PAPR lens; the inlet of the plastic tube was placed at the midpoint between the headform's mouth and bottom of the nose at ~1 cm from the headform's

surface; silicone sealant was used around the tube/lens interface location to prevent leaks (Fig 3).

During each test, differential pressure (to that of the laboratory room atmosphere) was measured using a multifunction meter (model: VelociCalc® Multi-Function Ventilation Meter 9565-P; TSI, Inc.) at a location ~2.5 cm in front of the opening of the mouth inside of the PAPR facepiece. Readings were measured in inch water column (in. WC) (resolution: 0.001 in. WC; accuracy: +/− 1% of reading +/− 0.005 in. WC) at the fastest sampling rate of the instrument, one reading per second.

Test Procedure

Prior to IL testing, an airflow test was performed for each PAPR model to quantify the flow rate of air delivered to the RIC. Each model was tested with its specified battery fully charged. The airflow test system incorporates a rotary vane pump (model: Spencer® Vortex® VB002, The Spencer Turbine Co., Windsor, CT 06095), voltage variable autotransformer (Staco Energy Products, Dayton, OH), and mass flowmeter (model: 300 series; Teledyne Hastings Instruments, Hampton, VA) (Fig 4 (a, b)). For loose-fitting hoods and facepieces, the RIC was donned on a headform and placed inside a sealed acrylic test chamber (24” × 24” × 24”). The PAPR blower was placed outside the chamber and its supply air hose was connected to the RIC by passing it through a port in the chamber wall. Modeling clay was then used to form an airtight seal between the supply air hose and the port. A pressure meter (model: 9565-P, TSI, Inc.) monitored the differential pressure (one sec sampling rate) of the chamber to that of the laboratory room via a port on top of the chamber. The airflow rate of the PAPR blower was determined by the mass flowmeter by starting the PAPR blower and rotary vane pump simultaneously and then adjusting the voltage of the rotary vane pump until the pressure meter read 0.000 in. WC differential pressure. Three trials were performed for each test. Because the blower motor is integral to the MaxAir® helmet, this model was donned onto a headform having a pressure tap inlet between the mouth and nose and also having a breathing tube running from the mouth and out of the back of the head; for this test, the headform was not placed inside the chamber. A hose was connected to the outlet of the headform’s breathing tube to the flowmeter’s inlet. Differential pressure was monitored on the inside of the PAPR RIC. Airflow was determined by adjusting the voltage of the rotary vane pump in the same manner described previously.

Testing using the HEPA-CONFIG setup was performed first. The sequence of work rates for IL testing for each PAPR model was randomly chosen. New PAPR HEPA filters were installed for each set of work rate tests. For each work rate, five 2-min tests were run in sequence on the same donning. First, the PAPR was donned on the headform and the blower was allowed to run for one minute without the breathing machine operating to flush any residual particles from the RIC. Next, the chamber door was closed and the NaCl aerosol introduced. Following the five tests at the first work rate, a new PAPR filter was installed prior to the first test of the next work rate. This process continued until all four sets of work rate testing were completed. The total test time for each PAPR model to complete IL testing of all four work rates was approximately 50 min. After completing testing of all four work rates, a posttest airflow test was performed. For the posttest airflow measurements, the

battery was not recharged nor was a new filter installed. After the posttest airflow measurements were made, batteries were charged for a minimum of 15 hours and testing was repeated in the same manner using the NO-HEPA-CONFIG setup.

Analysis

For each individual test, the average concentrations of the 2-min samples from each CPC were used to calculate the manikin penetration factor (mPF). Manikin penetration factor is the inverse of manikin total penetration (mTP). The term mTP is an accepted term by the American Industrial Hygiene Respiratory Protection Committee. The term mTP is defined as the fraction of an airborne challenge that enters a respirator mounted to a manikin from any source. The average 2-min concentration of the chamber sample [C_{out}] was divided by the average 2-min concentration of the in-mask sample [C_{in}]; (Equation 1). Statistical Analysis System (SAS) software Version 9.2 (SAS Institute Inc., Cary, N.C.) was used for all data analyses.

$$mPF = [C_{out}] / [C_{in}] \quad \text{(Equation 1)}$$

These calculated mPFs were then used to determine the geometric mean (GM), geometric standard deviation (GSD), and fifth percentile mPFs by each data grouping of model / work rate / IL test configuration (i.e., HEPA-CONFIG and NO-HEPA-CONFIG).

For each PAPR model of each IL test configuration, analysis of variance (ANOVA) tests using the PROC GLM command (general linear model) were performed on common logarithmically-transformed mPF values (LOGMPF) to test the dependence of LOGMPF on the independent variable work rate (WORKRATE) at the significance level (*P*-value) of 0.05; a Duncan's Multiple Range Test (DMRT) was tested on LOGMPF by PAPR model as a post hoc analysis to determine which work rate means were significantly different.

Additionally, two separate two-way ANOVA's (one ANOVA for each of the two different exhalation circuit configurations) were run to test the dependence of LOGMPF on the independent variables of PAPR model (MODEL) and WORKRATE and the interaction term MODEL*WORKRATE.

Finally, an ANOVA test was performed combing all test data from both exhalation circuit test configurations to test the dependence of LOGMPF on the independent variables of exhalation circuit test configuration (CONFIG), MODEL, and WORKRATE and all two-way interaction terms.

RESULTS

The PAPR airflow rates exceeded the minimum NIOSH certification requirement of 170 Lpm for all models and all pre- and post- IL tests (the posttest taking place after running continuous for approximately 50 min) (Table I). The rank order for airflow is Model B < Model A < Model C. For data collected in the HEPA-CONFIG phase of testing, mean

airflow rates for Model B, Model A, and Model C were 185 (SD 1.0), 205 (SD 7.0), and 227 (1.7), respectively. Similar results were observed for the NO-HEPA-CONFIG portion of testing (Table I). The greatest change in mean airflow rates post-testing was a decrease of 12 Lpm (211 Lpm pretest, 199 Lpm posttest) (−6 % change) observed for Model A in testing of the HEPA-CONFIG.

Manikin penetration factor results for HEPA-CONFIG are summarized in Table II. All tests were significant ($P < 0.05$) for the dependence of LOGMPF on WORKRATE for all models. Post hoc DMRT tests showed differences in mean LOGMPF values within each model, although from a practical standpoint, all GM mPF values were > 1,000 (indicating high performance). For Model B and Model A, REST has the lowest GM mPF, although one would expect that it would have the highest GM mPF because REST is the lowest minute ventilation.

For testing in the NO-HEPA-CONFIG, GM mPFs generally followed the expected trends based on work rate better than the HEPA-CONFIG (Table III). The HIGH work rate had the lowest GM mPF for all three models, although none of the models had REST as the work rate with the highest GM mPF. All tests were significant ($P < 0.05$) for the dependence of LOGMPF on WORKRATE for all models. Model B was the only model to have two work rates with the same DMRT grouping (LOW and REST) meaning that their mean mPFs were not significantly different. Comparing data for Model B in Tables II and III, the range of GM mPFs was similar for the first three rankings of GM mPF (HEPA-CONFIG: 5,110-5,770; NO-HEPA-CONFIG: 5,490-6,330), although the lowest ranking was quite different (HEPA-CONFIG (REST): 4,320; NO-HEPA-CONFIG (HIGH): 1,150). This trend pattern was similar for Model C where the first three GM mPFs rankings had a similar range (HEPA-CONFIG: 402,000-564,000; NOHEPA-CONFIG: 331,000-681,000) and the lowest GM mPF ranking had a large difference (HEPA-CONFIG (MODERATE): 310,000; NO-HEPA-CONFIG (HIGH): 22,000). For Model A, the entire range of GM mPFs was reduced when removing the in-line HEPA (HEPA CONFIG: 151,000–184,000; NO-HEPA-CONFIG: 30,000–123,000).

For the HIGH work rate results of the NO-HEPA-CONFIG (Table III), the GM mPFs for Model A and Model C were 30,000 (GSD 1.1) and 22,000 (GSD 1.1), respectively. The results are unexpected when comparing the two models; one would expect that the GM mPF using the HIGH work rate would have been greater for Model C because Model C had higher measured airflow rates compared to Model A (Table I). It is possible there was an unknown source of error in one or both of these sets of GM mPF measurements.

Summary data of mean in-mask pressure taken during the 2-min sampling period show that mean pressures for all models and work rates were positive (Fig. 5). For all work rates with the exception of HIGH, the ranking of mean pressure is Model B < Model A < Model C; however, for the HIGH work rate, the mean pressure is nearly equal for Model B (0.141 in. WC, SD 0.106) and Model A (0.117 in. WC, SD 0.022). Summary data of minimum in-mask pressures (the lowest pressure recorded over the 2-min test period for all tests) are presented in Fig. 6. For each model, the data follow the expected trend that the mean minimum pressure should correspond to work rate in the order HIGH < MODERATE <

LOW < REST. The mean minimum pressures were negative for the HIGH (−0.017 in. WC, SD 0.017) and MODERATE (−0.007 in. WC, SD 0.011) work rates for Model B. At HIGH work rate, Model A had mean minimum pressure of 0.000 (SD 0.016). None of the mean data were negative for Model C. It is not surprising that the order of mean minimum pressure for all work rates is Model C > Model A > Model B (Fig. 6) which corresponds to the same order of highest to lowest PAPR airflow rates summarized in Table I. The higher blower flow rates contributed to higher minimum in-mask pressures.

The ANOVA's performed separately for each exhalation cycle configuration show all independent variables and the interaction (MODEL, WORKRATE, and MODEL*WORKRATE) are significant effects ($P < 0.05$) for LOGMPF (Table IV). When data were combined for both exhalation cycle test configurations, significant effects were observed for the independent variables CONFIG, MODEL, WORKRATE and all two-way interactions between them (Table V).

DISCUSSION

PAPRs are used in healthcare when performing aerosol-generating procedures on high-risk patients, treating patients posing a risk of airborne infection, and administering certain hazardous aerosolized medications.(Liverman, Domnitz et al. 2014) The current estimate of more than 18 million United States healthcare workers emphasizes the need for effective personal protective equipment.(Centers for Disease Control, 2017) Our current study assessed performance of three common PAPR models used in healthcare to evaluate the current state of PAPR technology and as a preliminary effort to developing a manikin-based procedure.

PAPR model, work rate, and the exhalation circuit test configuration significantly affected PAPR performance. For all three models tested at all four work rates, GM mPFs and fifth percentile mPFs exceeded each model's OSHA APF; these results were observed for both IL chamber test conturations (HEPA-CONFIG and NO-HEPA-CONFIG). The results for HEPA-CONFIG testing for Model B and Model A infer that the in-line HEPA filter in the exhalation circuit caused a systematic error, likely diluting facepiece particle concentration at the LOW, MODERATE, and HIGH work rates in greater proportion to the REST work rate, as REST had the lowest GM mPF for these models. When using the in-line HEPA filter when testing the REST work rate, a relatively small volume of HEPA-filtered air (0.8 L) is returned to the RIC in the exhalation cycle compared to the larger volumes of the higher work rates. The higher work rate tests could have erroneously decreased GM mPFs due to a greater diluted in-mask particle concentration resulting from the larger exhaled volume (compared to the REST work rate). When using the in-line HEPA filter in the exhalation circuit, Model C followed the expected GM mPF trend (corresponding to work rate) reasonably well from highest to lowest mPF in the order of LOW, REST, HIGH, and MODERATE; these results may have been less affected by the returned (exhaled) filtered air (compared to the other two models) due to Model C's higher airflow rate (contributing to higher GM mPFs) compared to the other two models (Table I).

Previous studies evaluating the performance of different classes of respirators on headforms have utilized a single in-line HEPA filter in their test systems to filter the air both during inhalation and exhalation, but have not reported any abnormalities.(Grinshpun, Haruta et al. 2009, He, Grinshpun et al. 2014, Gao, McKay et al. 2016) Our study only passed the air through the filter on exhalation. By only passing air through the filter one way (as opposed to cyclically moving air through it), we avoided any possibility of returning particles back to the headform collected on the inhalation side of the filter. Due to the unexpected results obtained using the in-line HEPA filter, we are more confident in the results from the NO-HEPA-CONFIG configuration and future testing will be performed without an in-line filter. Although data from the NO-HEPA-CONFIG testing generally follows the expected trends better related to work rate, this configuration still carries the potential limitation of measuring an erroneously elevated particle concentration inside the RIC because the particles are returned to the RIC during exhalation.

Over breathing of PAPRs with loose-fitting RICS has been observed in previous studies by measuring the in-mask pressure differential.(da Roza, Cadena-Fix et al. 1990, Cohen, Hecker et al. 2001, Mackey, Johnston et al. 2005, Sinkule, Powell et al. 2016) Despite observing negative pressures in our study for the HIGH work rate (all three models) and MODERATE work rate (Model B only), high mPFs (both GM and fifth percentile values) were observed (Table III). Although the mPFs for the three models in this study cannot be directly translated to user protection in the workplace, they do imply that even at a high work rates, these models remain highly efficient.

Future studies will use a pressure meter with a faster sampling rate in order to determine peak inhalation flow rates and their relationship to in-mask differential pressure. PAPR airflow rate at varied levels will also be studied to determine the effect on PAPR performance. Future studies will also be performed using a robotic headform to simulate head and facial movements including head turning and nodding and mimicking the mouth movements of speech. These types of studies may be able to determine which exercises create the greatest amount of inward leakage. Further development of a manikin-based method should incorporate the four work rates chosen for this study (or of a similar range) to provide a challenging test. Our study did not monitor PAPR airflow delivery rate during the IL testing as was done in previous studies;(Cohen, Hecker et al. 2001, Koh, Johnson et al. 2011) however, this can be done in future testing to correlate PAPR airflow rate with the IL for each exercise.

Limitations

This study evaluated only a small number (3) of PAPR models. Testing of additional loose-fitting as well as tight-fitting models will acquire better knowledge of the current state of PAPR product performance. The pressure meter used in this study only sampled at 1 reading/second, thus it is possible that the peak inhalation pressure was missed. Future evaluations should utilize a meter with a faster sampling rate. Filtration efficiency of each model’s PAPR filter was not evaluated in this study. Slight variations in filter performance, mounting the PAPR on the headform, or the exact fitting of the filter into the PAPR may have contributed to inward leakage. These parameters can be assessed in future studies.

CONCLUSIONS

The PAPR model, work rate, and test configuration were observed to affect PAPR performance. Testing of all three PAPR models resulted in geometric mean and fifth percentile mPFs greater than their designated OSHA APFs. Advanced headforms have potential for assessing PAPR performance once test methods can be matured. A manikin-based inward leakage test method for PAPRs can be further developed using the knowledge gained from this study. Additional future research is needed to evaluate the correlation of PAPR performance using advanced headforms to the performance measured with human subjects.

Acknowledgements

The authors would like to thank our NIOSH colleagues Raymond Roberge, William King, and Jeffrey Palcic who provided their review and input to the manuscript.

REFERENCES

Adams WC (1993). Measurement of breathing rate and volume in routinely performed daily activities. Final report. California Air Resources Board, California Environmental Protection Agency: Contract No. A033–205.

Ainsworth BE, Haskell WL, Herrmann SD, et al. (2011) 2011 Compendium of Physical Activities: a second update of codes and MET values. Med. Sci. Sports Exerc. 43(8): 1575–1581. [PubMed: 21681120]

Anderson NJ, Casidy PE, Janssen LL, et al. (2006). Peak inspiratory flows of adults exercising at light, loderate and heavy work Loads. J. Int. Soc. Resp. Protect. 23(Spring-Summer): 53–63.

Bergman M, He X, Joseph M, et al. (2015). Correlation of respirator fit measured on human subjects and a static advanced headform. J. Occup. Environ. Hyg. 12(3): 163–171. [PubMed: 25265037]

Bergman M, Zhuang Z, Hanson D, et al. (2014). Development of an advanced respirator fit-test headform. J. Occup. Environ. Hyg. 11(2): 117–125. [PubMed: 24369934]

Berndtsson G (2004). Peak inhalation air flow and minute volumes measured in a bicycle ergometer test. J. Int. Soc. Resp. Protect. 21(1–2): 21–29.

Bureau of Labor Statistics and National Institute for Occupational Safety and Health (2003). Respirator Usage in Private Sector Firms, 2001.

Caretti D, and Coyne K (2004). Workplace Breathing Rates: Defining Anticipated Values and Ranges for Respirator Certification Testing, Report No. ECBC-TR-316, Edgewood Chemical Biological Center, U.S. Army Research, Development and Engineering Command.

Centers for Disease Control (2017). Workplace safety and health topics: Healthcare workers. http://www.cdc.gov/niosh/topics/healthcare (accessed June 01, 2017). Page last review January 2017.

Cohen H, Hecker L, Mattheis D, et al. (2001). Simulated workplace protection factor study of powered air-purifying and supplied air respirators. Am. Ind. Hyg. Assoc. J. 62: 595–604.

da Roza R, Cadena-Fix C, and Kramer J (1990). Powered air-purifying respirator study. J. Int. Soc. Resp. Protect. 8(2): 15–36.

Federal Register (1995). National Institute for Occupational Safety and Health (NIOSH), Respiratory Protective Devices. Washington, DC, US Government Printing Office, Office of the Federal Register. 42 CFR Part 84.

Gao S, McKay R, Yermakov M, et al. (2016). Performance of an improperly sized and stretched-out loose-fitting powered air-purifying respirator: Manikin-based study. J. Occup. Environ. Hyg. 13(3): 169–176. [PubMed: 26554716]

Grinshpun S, Haruta H, Eninger R, et al. (2009). Performance of an N95 filtering facepiece particulate respirator and a surgical mask during human breathing: two pathways for particle penetration. J. Occup. Environ. Hyg. 6(10): 593–603. [PubMed: 19598054]

He X, Grinshpun S, Reponen T, et al. (2014). Effects of Breathing Frequency and Flow Rate on the Total Inward Leakage of an Elastomeric Half-Mask Donned on an Advanced Manikin Headform. Ann. Occup. Environ. Hyg. 58(2): 182–194.

ILC Dover, LP (2011). Assigned Protection Factor Determination For: Sentinel XL Powered Air Purifying Respirator with Sentinel XL Full Hood. Conducted by: Laboratory Respirator Protection Level Facility, ILC Dover LP. Report obtained from ILC Dover, LP.

Janssen L, Anderson N, Cassidy P, Weber R, and Nelson T (2005). Interpretation of inhalation airflow measurements for respirator design and testing. J. Int. Soc. Resp. Protect. 22(Fall-Winter 2005): 122–141.

Khoo K, Leng P, Ibrahim I, and Lim T (2005). The changing face of healthcare worker perceptions on powered air-purifying respirators during the SARS outbreak. Respirology. 10(1): 107–110. [PubMed: 15691247]

Koh F, Johnson A, and Rehak T (2011). Inward leakage in tight-fitting PAPRs. J. Environ. Public Health. Article ID 473143, http://downloads.hindawi.com/journals/jeph/2011/473143.pdf. (accessed June 01, 2017).

Koivisto A, Aromaa M, Koponen I, et al. (2015). Workplace performance of a loose-fitting powered air purifying respirator during nanoparticle synthesis. J. Nano. Res. 17(4): 177.

Liverman C, Domnitz S, and McCoy M (2014). The use and effectiveness of powered air purifying respirators (PAPRs) in health care Institute of Medicine of the National Academies of Science, Washington, DC. .

Mackey R, Johnston A, Scott W, et al. (2005). Over breathing a loose-fitting PAPR. J. Int. Soc. Resp. Protect. 22: 1–10.

Martin S, Moyer E, and Jensen P (2006). Powered, air-purifying particulate respirator filter penetration by a DOP aerosol. J. Occup. Environ. Hyg. 3(11): 620–630. [PubMed: 17086666]

National Institute for Occupational Safety and Health (NIOSH) (2005). NIOSH Respirator Selection Logic 2004. Cincinnati, U.S. Department of Health and Human Services, Centers for Disease Control and Prevention, Department of Health and Human Services, NIOSH. Publication No. 2005–100.

Occupational Safety and Health Administration (OSHA) (1998). Respiratory Protection. Washington, DC, US Government Printing Office, Office of the Federal Register. 29 CFR 1910.134.

Occupational Safety and Health Administration (OSHA) (2006). Assigned Protection Factors: Final rule. 29 CFR Parts 1910, 1915, 1926 71: 50121–50192 http://www.osha.gov/pls/oshaweb/owadisp.show_document?p_table=FEDERAL_REGISTER&p_id=18846. (accessed June 01, 2017)

Sinkule E, Powell J, Rubenstein E, et al. (2016). Physiologic effects from using tight- and loose-fitting powered air-purifying respirators on inhaled gases, peak pressures, and inhalation temperatures during rest and exercise. J. Int. Soc. Resp. Protect. 33(2): 36–52.

Wizner KL, Stradtman L, Novak D, and Shaffer R (2016). Prevalence of respiratory protective devices in U.S. health care facilities: Implications for emergency preparedness. Work. Health Saf. 64(8): 359–368.

Zhuang Z, Benson S, and Viscusi D (2010). Digital 3-D headforms with facial features representative of the current US workforce. Ergonomics. 53(5): 661–671. [PubMed: 20432086]

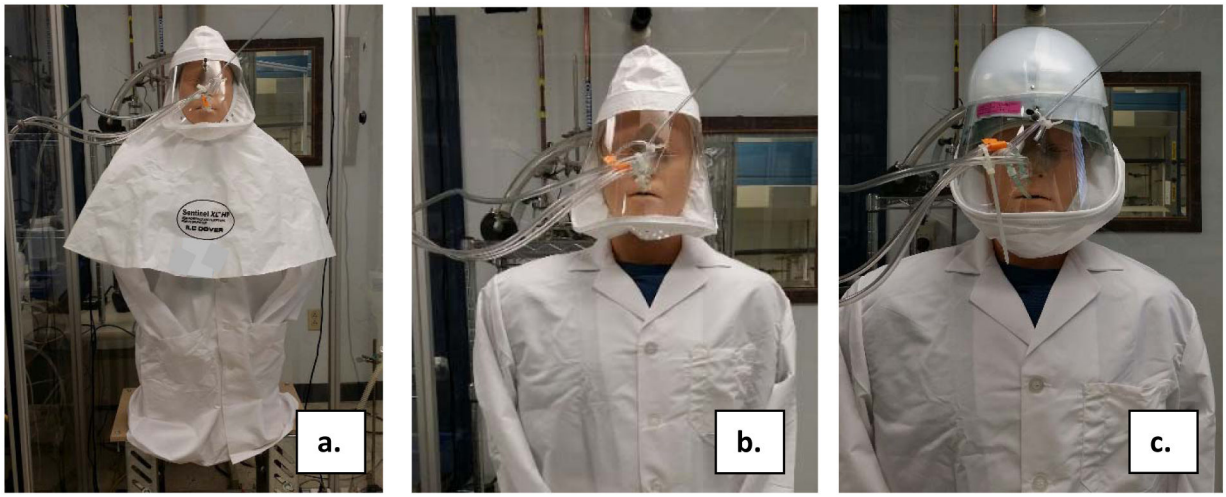

Figure 1. PAPR Models.

a.) Sentinel XL^{TM} with S-2019-10 hood (one size only)

b.) 3M Air-Mate^{TM} with model BE-12 facepiece (size Regular) (3M Company, St. Paul, MN)

c.) MaxAir$^{®}$ 78SP-36 cuff system with disposable cuff (size ML) (Bio-Medical Devices, Inc., Irvine, CA) (credits for all photos: NIOSH)

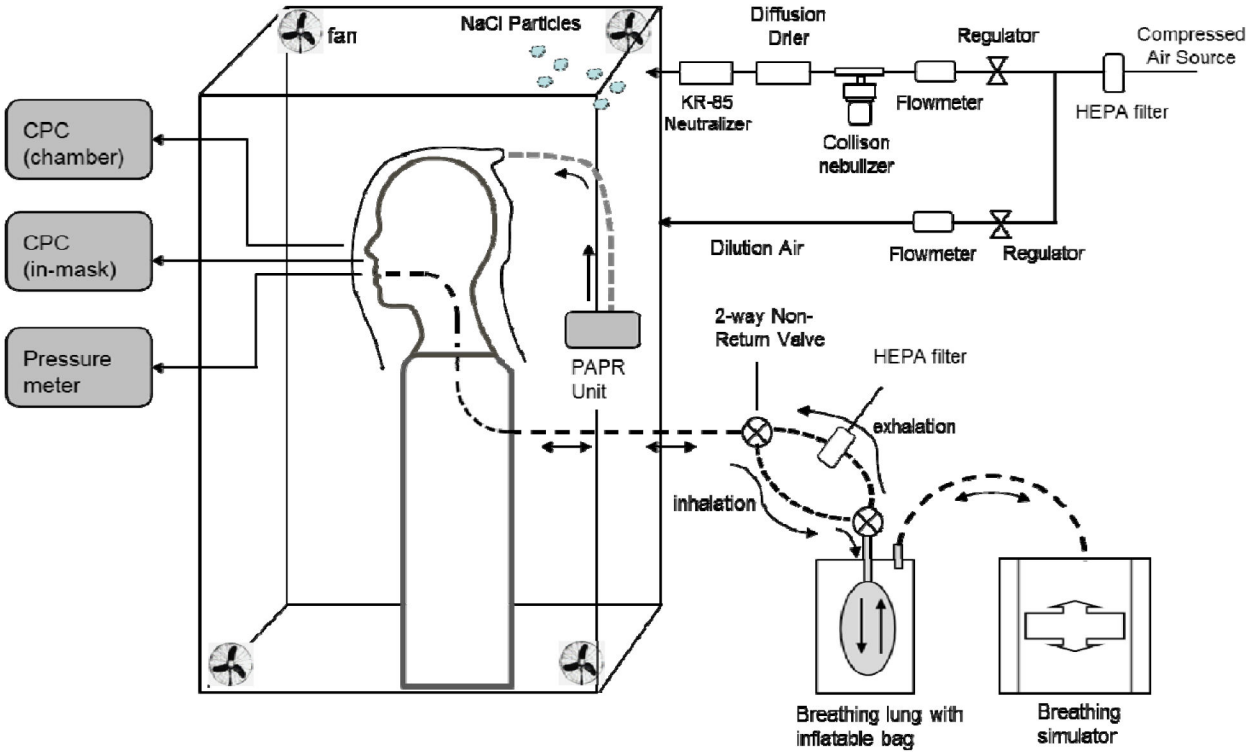

Figure 2.
Experimental set up for PAPR inward leakage testing.

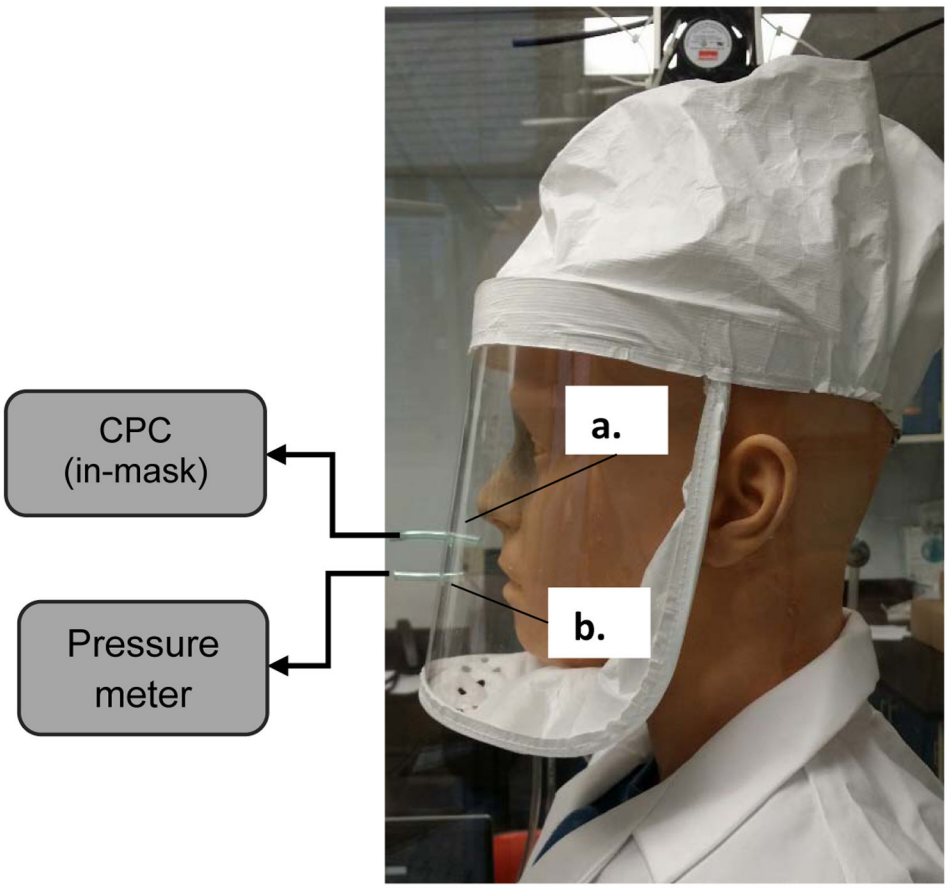

Figure 3. Placement of in-mask sampling tubes.

a. Sample tube extending into facepiece for particle sampling. The inlet was located ~1 cm from the headform's surface at the point midway between the bottom of the nose and upper lip.

b. Sample tube extending into facepiece for differential pressure measurement. The inlet was located ~2.5 cm in front of mouth opening (photo credit: NIOSH).

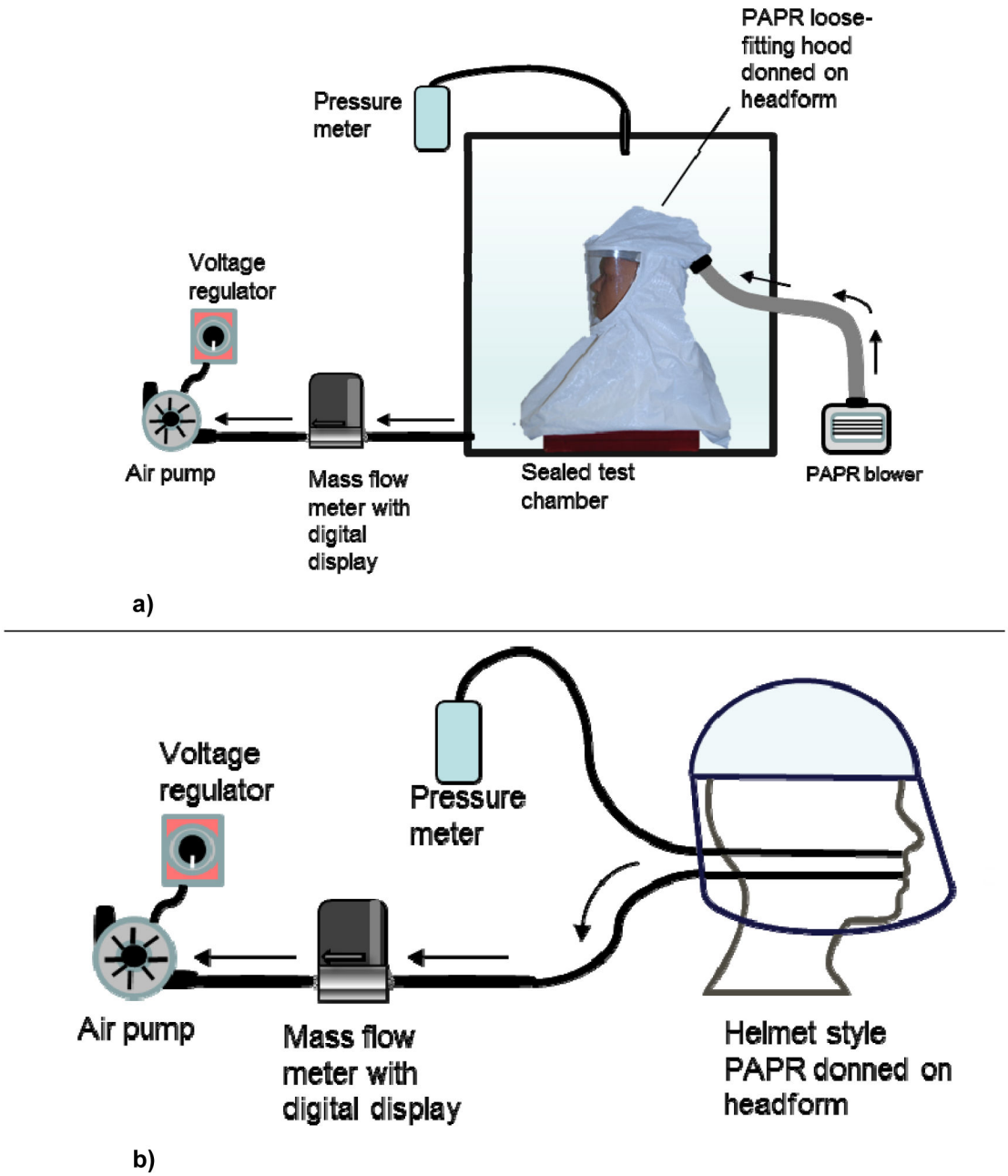

Figure 4.

Airflow Test System for a) Loose-fitting hood and facepiece style PAPRs and b) Loose-fitting helmet style PAPRs.

Workrate												
high			moderate			low			rest			
Pressure												
n	10	10	10	10	10	10	10	10	10	10	10	10
mean	0.117	0.141	0.427	0.111	0.039	0.322	0.111	0.102	0.239	0.117	0.082	0.236
sd	0.022	0.106	0.047	0.015	0.002	0.002	0.017	0.072	0.034	0.018	0.045	0.010
min	0.095	0.037	0.381	0.094	0.035	0.318	0.093	0.029	0.178	0.099	0.037	0.224
max	0.138	0.244	0.479	0.126	0.041	0.325	0.131	0.172	0.270	0.140	0.127	0.246

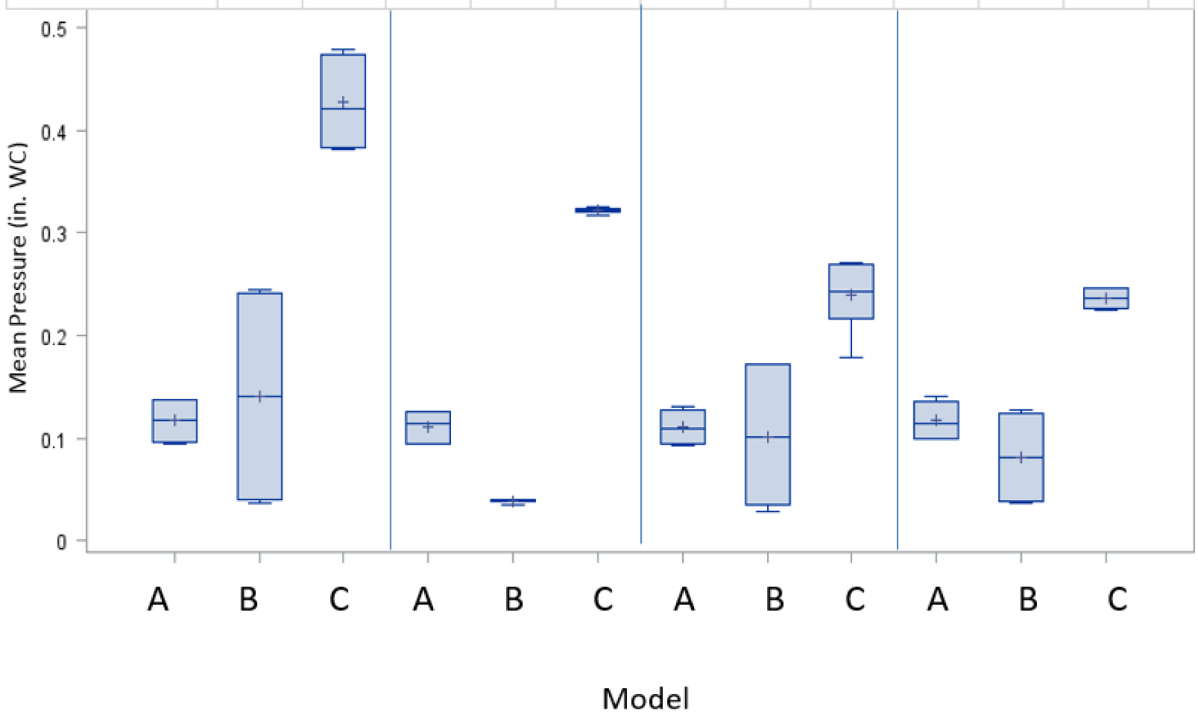

Figure 5.
Summary of Mean In-mask Pressures.

Workrate	high			moderate			low			rest		
Pressure												
n	10	10	10	10	10	10	10	10	10	10	10	10
mean	-0.000	-0.017	0.002	0.016	-0.007	0.063	0.049	0.008	0.131	0.084	0.051	0.175
sd	0.016	0.017	0.037	0.010	0.011	0.027	0.010	0.014	0.005	0.013	0.038	0.014
min	-0.024	-0.039	-0.052	0.001	-0.024	0.029	0.034	-0.018	0.121	0.068	0.006	0.152
max	0.020	0.003	0.037	0.031	0.005	0.105	0.063	0.031	0.137	0.105	0.091	0.189

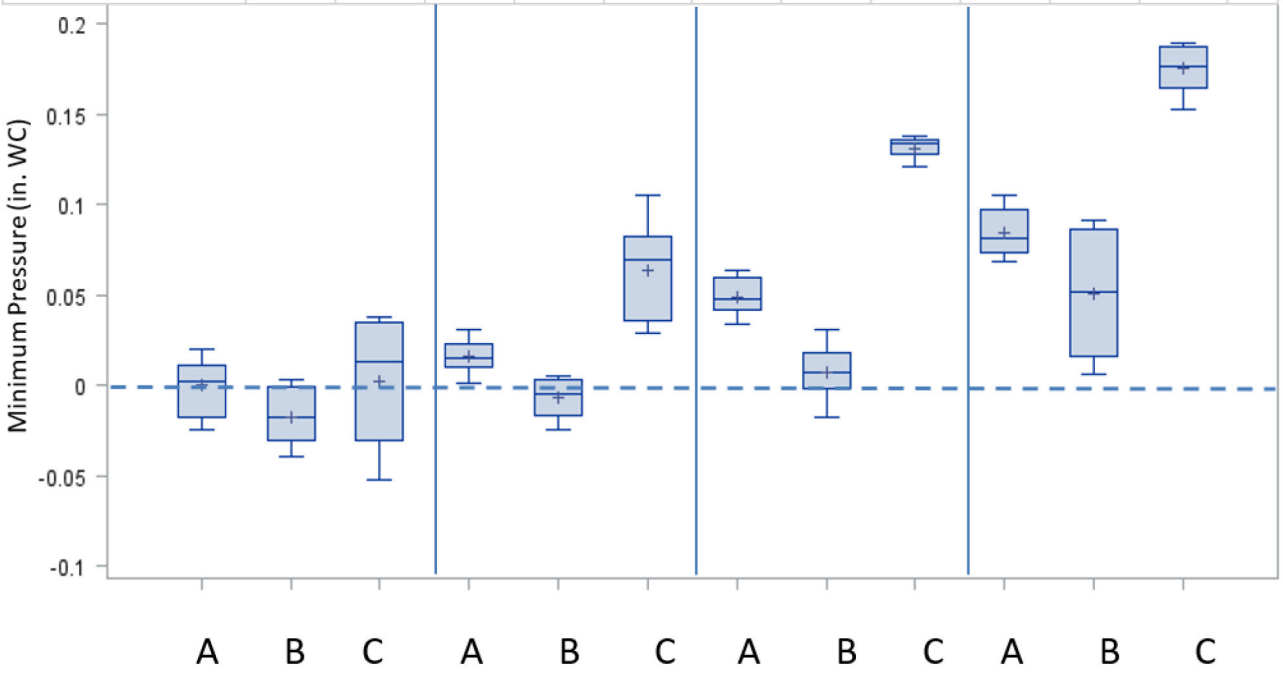

Figure 6.
Summary of Minimum In-mask Pressures.

Table I.

PAPR Airflow Rates Measure Pre- and Post- Inward Leakage (IL) Testing

Model	n (tests)	Pretest Mean Airflow (Lpm)	SD	n (tests)	Posttest Mean Airflow (Lpm)	SD	Δ Airflow Pre-Post (Lpm) (%)	n (tests)	All Mean Tests	SD
Airflow measurements for HEPA-CONFIG testing										
A	3	211	2.5	3	199	1	12 (−6 %)	6	205	7.0
B	3	186	1	3	185	0.6	1 (−1 %)	6	185	1.0
C	3	228	2	3	226	1.2	2 (−1 %)	6	227	1.7
Airflow measurements for NO-HEPA-CONFIG testing										
A	3	218	0.6	3	208	1.2	10 (−5 %)	6	213	5.2
B	3	187	0.6	3	184	0.6	3 (−2 %)	6	185	1.7
C	3	235	1	3	234	0.6	1 (< −1 %)	6	234	1.0

Table II.

Manikin Penetration Factor (mPF) Results: With In-line-HEPA Filter in Breathing Pathway (HEPA-CONFIG)

Model	Work Rate	n (tests)	GM mPF	GSD	5th Percentile mPF	*P*-value[2]	Duncan's Grouping
A	MODERATE	5	184,000	1.0	171,000	**<0.05**	A
	LOW	5	168,000	1.1	145,000		B
	HIGH	5	152,000	1.1	140,000		C
	REST	5	151,000	1.1	136,000		C
B	LOW	5	5,770	1.0	5,710	**<0.05**	A
	MODERATE	5	5,110	1.0	4,900		B
	HIGH	5	5,110	1.1	4,600		B
	REST	5	4,320	1.0	4,200		C
C	LOW	5	564,000	1.1	515,000	**<0.05**	A
	REST	5	540,000	1.1	496,000		A
	HIGH	5	402,000	1.0	379,000		B
	MODERATE	5	310,000	1.1	284,000		C

[1] For MaxAir®, MODERATE and HIGH work rates had equal GM mPF values (5,110).

[2] Determined for ANOVA model with dependent variable LOGMPF and independent variable WORKRATE.

Table III.

Manikin Penetration Factor (mPF) Results: Without In-line-HEPA Filter in Breathing Pathway (NO-HEPA-CONFIG)

Model	Work Rate	n (tests)	GM mPF	GSD	5th Percentile mPF	*P*-value[1]	Duncan's Grouping
A	MODERATE	5	123,000	1.0	114,000	**<0.05**	A
	LOW	5	105,000	1.0	98,100		B
	REST	5	97,900	1.1	87,700		C
	HIGH	5	30,000	1.1	27,700		D
B	LOW	5	6,330	1.0	5,960	**<0.05**	A
	REST	5	6,220	1.0	6,100		A
	MODERATE	5	5,490	1.0	5,420		B
	HIGH	5	1,150	1.1	961		C
C	MODERATE	5	681,000	1.1	557,000	**<0.05**	A
	REST	5	419,000	1.1	353,000		B
	LOW	5	331,000	1.1	302,000		C
	HIGH	5	22,000	1.1	18,500		D

[1]Determined for ANOVA model with dependent variable LOGMPF and independent variable WORKRATE.

TABLE IV.

ANOVA Results by Exhalation Circuit Configuration

Source[1]	DF	Sum of Squares	Mean Square	F Value	P-value[2]
Using In-line HEPA Filter (HEPA-CONFIG)					
MODEL	**2**	**41.57**	**20.79**	**41751.2**	**<0.05**
WORKRATE	**3**	**0.07**	**0.02**	**49.7**	**<0.05**
MODEL*WORKRATE	**6**	**0.21**	**0.04**	**71.2**	**<0.05**
Without Using In-line HEPA Filter (NO-HEPA-CONFIG)					
MODEL	**2**	**32.51**	**16.26**	**15517.8**	**<0.05**
WORKRATE	**3**	**8.43**	**2.81**	**2681.28**	**<0.05**
MODEL*WORKRATE	**6**	**1.37**	**0.23**	**218.12**	**<0.05**

1. MODEL=PAPR model, WORKRATE=work rate.

2. Determined for dependent variable LOGMPF.

TABLE V.

ANOVA Results For All Data Combined

Source[1]	DF	Sum of Squares	Mean Square	F Value	P-value[2]
CONFIG	**1**	**1.81**	**1.81**	**193.16**	**<0.05**
MODEL	**2**	**73.79**	**36.89**	**3942.77**	**<0.05**
WORKRATE	**3**	**4.47**	**1.49**	**159.35**	**<0.05**
CONFIG*MODEL	**2**	**0.30**	**0.15**	**15.82**	**<0.05**
WORKRATE*CONFIG	**3**	**4.03**	**1.34**	**143.45**	**<0.05**
WORKRATE*MODEL	**6**	**0.70**	**0.12**	**12.53**	**<0.05**

1. CONFIG=exhalation circuit configuration, MODEL=PAPR model, WORKRATE=work rate.

2. Determined for dependent variable LOGMPF.